JOURNAL OF THERMOPHYSICS AND HEAT TRANSFER
Vol. 8, No. 4, Oct.–Dec. 1994

Review of Elastic and Plastic Contact Conductance Models: Comparison with Experiment

M. R. Sridhar* and M. M. Yovanovich†
University of Waterloo, Waterloo, Ontario N2L 3G1, Canada

More than 450 thermal contact conductance data points obtained from isotropic conforming rough surfaces for five different materials; nickel, stainless steel, two zirconium alloys, and aluminum have been compared with the existing elastic and plastic models. For the first time data have been reduced to a dimensionless form assuming both elastic as well as plastic deformation. Normally, data were compared with either the elastic model or the plastic model assuming a type of deformation a priori. The relative merits of different models and the surface factors influencing the mode of deformation are still not clear. Hence, the aim of the present work was to compare most of the models available in the literature with themselves as well as with isotropic data. Comparison showed that generally smoother surfaces deform elastically, and rougher ones plastically. However, there are some data sets that compare well with both the elastic as well as the plastic models.

Nomenclature

A_a, A_r = apparent, real contact area, m^2
a = mean circular contact radius, m
C = dimensionless asperity curvature $\equiv l^2/(\beta\sigma)$
c_1, c_2 = Vickers correlation coefficients, c_1, MPa
D = fractal dimension of the surface profile
D_{sum} = total number of summits/unit apparent area, m^{-2}
d_V = Vickers indentation diagonal, μm
E, E' = elastic modulus, equivalent elastic modulus, MPa
$f(\lambda)$ = function used in the Bush, Gibson, and Thomas model
$g(D, A_r/A_a)$ = some function of D and A_r/A_a
H, H_c = bulk hardness, contact microhardness, MPa
h_c = contact conductance, $W/m^2 \cdot K$
I_v^{-1}, $I_{v,w}^{-1}$, $f^{-1}(\lambda)$ = inverse functions used in the text
$I_v(\lambda)$ = integral used in the Greenwood and Williamson model
$I_{v,w}(\lambda)$ = double integral used in the Whitehouse and Archard model
k_s = harmonic mean thermal conductivity, $W/m \cdot K$
l = sampling interval, m
m = effective mean absolute surface slope, rad
m_0 = variance of surface heights, μm^2
m_2 = variance of surface slopes, rad^2
m_4 = variance of the second derivative of surface heights, μm^{-2}
n = number/unit apparent area, m^{-2}
P = force/unit apparent area, MPa
Q = heat transfer rate, W
S_f = material yield or flow stress, MPa
s = dimensionless variable, $\equiv y/\sigma$
T_c = mean interface temperature, °C
Y = surface mean plane separation, m
α = bandwidth parameter, $\equiv (m_0 m_4/m_2^2)$
β = radius of curvature of summits, m
ΔT_c = effective temperature drop across the interface, °C
η = load-exponent for contact area-load relation
λ = dimensionless surface mean plane separation, $\equiv Y/\sigma$
ν = Poissons ratio
σ = rms surface roughness heights for given surface pair, m
σ^* = dimensionless roughness parameter

Subscripts
A, B = surfaces A and B
a = apparent area
c = contact
r = real area
θ = slope

Received Oct. 8, 1993; revision received March 22, 1994; accepted for publication March 25, 1994.

*Graduate Research Assistant, Microelectronics Heat Transfer Laboratory, Department of Mechanical Engineering. Student Member AIAA.

†Professor and Director, Microelectronics Heat Transfer Laboratory, Department of Mechanical Engineering. Fellow AIAA.

Introduction

OVER the past 25 yr a number of contact conductance models have been proposed for two conforming rough surfaces in contact under load. The contact conductance model is a combination of three models: 1) the thermal model, 2) the surface geometry model, and 3) the deformation model. The thermal model that predicts the contact conductance needs the surface geometry model and the deformation model to estimate the contact spot density and the size of each contact.

Most of the surface geometry models for isotropic rough surfaces assume circular contact spots and use probability theory to predict contact spot parameters such as the contact spot density, ratio of real area to the apparent area, and the applied load. The differences observed between various contact conductance models are essentially in their surface geometry model. The surface geometry model in turn needs a deformation model. There are two deformation models available for frictionless circular contact, viz., 1) the Hertz[1] elastic model and 2) the geometric plastic model. Depending upon the type of deformation model used, the contact conductance model becomes either an elastic model or a plastic model.

The aim of this article is to review most of the elastic and plastic models available in the literature and to compare these contact conductance models with experimental data obtained

for isotropic similar materials by Antonetti,[2] Hegazy,[3] and McWaid.[4]

Review of Elastic and Plastic Contact Conductance Models

Most of the contact conductance models reviewed here differ only in the surface geometry part of their model. The models presented in this section are for isotropic rough surfaces, i.e., the models assume no variations in surface profile slopes with direction. Also, the contact stresses depend only upon the relative profile of their two surfaces. Therefore, the system of two rough surfaces in contact can be replaced by a single flat rigid surface in contact with a body having an effective modulus $E' = [(1 - \nu_A^2)/E_A + (1 - \nu_B^2)/E_B]^{-1}$, equivalent roughness $\sigma = \sqrt{\sigma_A^2 + \sigma_B^2}$, and mean absolute slope $m = \sqrt{m_A^2 + m_B^2}$.

The surface models do not differentiate between profile and surface statistics, whereas in the modified surface model presented by McWaid and Marschall,[5] the surface statistics and profile statistics are considered different. In the modified model the mean summit plane and surface plane do not coincide and the summit plane is above the surface mean plane. The surface parameters for both the unmodified and modified surface models are given by

density of the summits

$$D_{\text{sum}} = (1/\mathcal{A})(m_4/m_2) \tag{1}$$

variance of surface heights

$$\sigma^2 = \mathcal{B} \cdot m_0 \tag{2}$$

radius of curvature of summits

$$\beta = (\mathcal{C}/\sqrt{m_4}) \tag{3}$$

where $m_2 = m_{2A} + m_{2B}$ and $m_4 = m_{4A} + m_{4B}$ are the variance of the surface slopes and the variance of the second derivative of the surface heights, respectively, for a surface pair. The constants $\mathcal{A}$, $\mathcal{B}$, $\mathcal{C}$ are 39.48 or 32.65; 1 or $(1 - 0.8968/\alpha)$; 0.798 or 0.665 for the surface model or the modified surface model, respectively, where $\alpha = m_0 m_4/m_2^2$ is called the bandwidth parameter.

The thermal model that predicts the contact conductance used in most of the models was first presented by Cooper, Mikic, and Yovanovich[6] (CMY). The contact conductance h_c for a surface pair is given by

$$h_c = [2k_s na/(1 - \sqrt{A_r/A_a})^{1.5}] \tag{4}$$

where the contact spot density n, contact spot radius a, and the ratio real area to apparent area A_r/A_a are obtained from the surface and deformation models.

The results of analyses of various elastic and plastic models, viz., the ratio of real area to apparent area, contact spot density, mean contact spot size, and contact conductance will be presented in this section.

Greenwood and Williamson[7] (GW) Model

In the GW model the asperity peaks are assumed to possess a Gaussian distribution about some mean reference plane and are hemispherically dome-shaped near their tips. Results of the GW elastic and plastic models are summarized in Table 1. The integral used in the GW model is given by

$$I_\nu(\lambda) = \frac{1}{\sqrt{2\pi}} \int_\lambda^\infty (s - \lambda)^\nu \exp(-s^2/2)\, ds \tag{5}$$

CMY and Mikic[8] Models

The contact conductance model for conforming rough surfaces undergoing plastic deformation developed by CMY[6] was based on isotropic surfaces having no variations in surface profile heights and slopes with direction. The model assumes that distributions of surface profile and slopes are Gaussian. Mikic,[8] on the basis of previous work by CMY[6] and by assuming that the elastic contact area is exactly half the plastic contact area, derived the elastic contact conductance model. Table 2 shows the Mikic and CMY models.

Table 1 GW elastic and plastic model

Deformation	Results
Elastic or plastic	$\frac{A_r}{A_a} = \kappa^a \pi D_{\text{sum}} \sigma \beta I_1(\lambda)$
	$n = \frac{1}{2} D_{\text{sum}} \operatorname{erfc}(\lambda/\sqrt{2})$
	$a = \sqrt{\frac{2\kappa^a \sigma \beta I_1(\lambda)}{\operatorname{erfc}(\lambda/\sqrt{2})}}$
	$h_c = \frac{\sqrt{2\kappa^a} k_s D_{\text{sum}} \sqrt{\operatorname{erfc}(\lambda/\sqrt{2})\sigma\beta I_1(\lambda)}}{[1 - \sqrt{\kappa^a \pi D_{\text{sum}} \sigma \beta I_1(\lambda)}]^{1.5}}$
Elastic	$\lambda = I_{3/2}^{-1}[3P/(4D_{\text{sum}} E' \sigma \sqrt{\sigma\beta})]$
Plastic	$\lambda = I_1^{-1}[P/(5.52\pi D_{\text{sum}} S_f \sigma\beta)]$

[a] $\kappa = 1$ for elastic, $\kappa = 2$ for plastic.

Table 2 Mikic/CMY elastic and plastic model

Deformation	Results
Elastic or plastic	$\frac{A_r}{A_a} = \frac{\kappa^a}{4} \operatorname{erfc}(\lambda/\sqrt{2})$
	$n = \frac{1}{16} \left(\frac{m}{\sigma}\right)^2 \frac{\exp(-\lambda^2)}{\operatorname{erfc}(\lambda/\sqrt{2})}$
	$a = \frac{2\sqrt{\kappa^a}}{\sqrt{\pi}} \frac{\sigma}{m} \exp(\lambda^2/2) \operatorname{erfc}(\lambda/\sqrt{2})$
	$h_c = \frac{\sqrt{\kappa^a} k_s}{4\sqrt{\pi}} \frac{m}{\sigma} \frac{\exp(-\lambda^2/2)}{[1 - \sqrt{(\kappa^a/4)\operatorname{erfc}(\lambda/\sqrt{2})}]^{1.5}}$
Elastic	$\lambda = \sqrt{2} \operatorname{erfc}^{-1}[4\sqrt{2}P/(E'm)]$
Plastic	$\lambda = \sqrt{2} \operatorname{erfc}^{-1}(2P/H_c)$

[a] $\kappa = 1$ for elastic, $\kappa = 2$ for plastic.

Table 3 BGT asymptotic elastic model

Deformation	Results
Elastic	$\frac{A_r}{A_a} = \frac{1}{2\sqrt{2\pi}} \frac{\exp(-\lambda^2/2)}{\lambda}$
	$n = \frac{1}{4\pi^2} \frac{m_2}{m_0} \exp(-\lambda^2/2)$
	$a = \sqrt{[(2\pi)^{1/2}/\lambda] \cdot (m_0/m_2)}$
	$h_c = \frac{\frac{k_s}{2^{3/4}\pi^{7/4}} \sqrt{(m_2/m_0)} \cdot \exp(-\lambda^2/2)/\sqrt{\lambda}}{\{1 - \sqrt{1/(2\sqrt{2\pi})}[\exp(-\lambda^2/2)/\lambda]\}^{1.5}}$
	$\lambda = f^{-1}[P2\sqrt{2}\pi/(E'\sqrt{m_2})]$

Bush, Gibson, and Thomas[9] (BGT) Asymptotic Elastic Model

The BGT asymptotic elastic model was presented in a convenient form by Sayles and Thomas.[10] This is applicable to isotropically rough surfaces with Gaussian height distributions. It is an asymptotic model and valid only when the dimensionless separation $\lambda \geq 2$. The BGT is presented in Table 3. The function used in the BGT elastic model $f(\lambda) = \exp(-\lambda^2/2)/\lambda$.

Whitehouse and Archard[11] (WA) Elastic Model

WA proposed a model for isotropic rough surfaces in contact. The WA model differs from the GW model in the fol-

Table 4 WA elastic model

Deformation	Results
Elastic	$\frac{A_r}{A_a} = \frac{\pi}{5} I_{1,1}(\lambda)$
	$n = \frac{i_{0,0}(\lambda)}{5l^2}$
	$a = l\sqrt{[I_{1,1}(\lambda)/I_{0,0}(\lambda)]}$
	$h_c = \frac{2k_s}{5l} \cdot \frac{\sqrt{I_{0,0}(\lambda)I_{1,1}(\lambda)}}{[1 - \sqrt{(\pi/5)I_{1,1}(\lambda)}]^{1.5}}$
	$\lambda = I^{-1}_{3/2,1/2}[15lP/(4E'\sigma)]$

lowing way: 1) the distribution of peaks is not quite Gaussian, but follows a distribution derived from assumed Gaussian distribution of heights; and 2) the peak curvatures have a distribution that is dependent upon the heights. Onions and Archard[12] have presented the WA model in a convenient form and have evaluated all the integrals used in the model. Results of the WA elastic is summarized in Table 4. The double integral used in the WA model is

$$I_{v,w}(\lambda) = \int_{\lambda}^{\infty} (s - \lambda)^v \int_0^{\infty} \frac{3\phi^*(s, C)}{C^w} \, dC \, ds \tag{6}$$

where

$$\phi^*(s, C) = \frac{\exp(-s^2/2)}{2\pi\sqrt{2}} \exp[-(s - C/2)^2]\text{erf}(C/2) \tag{7}$$

v	w
1	1
0	0
$\frac{3}{2}$	$\frac{1}{2}$

Majumdar and Tien[13] (MT) Model

MT have proposed a fractal network model for contact conductance. This model is very different from the other models presented in this section. The contact conductance is given by the expression

$$h_c = \frac{\sigma}{k_s} \frac{1}{g[D, (A_r/A_a)]\sqrt{4 - 2D}} \left[\frac{(2 - D)A_r/A_a}{D}\right]^{(D/2)} \tag{8}$$

where $D \equiv$ fractal dimension of the surface profile, and $g(D, A_r/A_a) \equiv$ some function of D, A_r/A_a (see Ref. 14). Contact mechanics of fractal surfaces by Majumdar and Bhushan[14] has shown that

$$(A_r/A_a) \sim (P/H)^{\eta} \tag{9}$$

where

$\eta \equiv$ area-load exponent ($\simeq$1–1.33), when
$D = 1$, $\eta = 1.0$, deformation is plastic
$D = 1.5$, $\eta = 1.33$, deformation is elastic
$D = 2.0$, $\eta = 1.0$, deformation is plastic

Comparison of the Elastic and Plastic Conductance Models with Data

Dimensionless Elastic and Plastic Contact Pressure

The first task was that of comparing different models undergoing a particular type deformation on a single plot. Hence, there was need for common dimensionless y and x axes parameters, i.e., the dimensionless contact conductance and the dimensionless contact pressure. It is known from the CMY[6] work that the ratio of applied pressure P to the contact hardness H of the softer material in contact is the most suitable dimensionless contact pressure parameter for two surfaces undergoing plastic deformation. It was later shown by Yovanovich and Hegazy[15] that an appropriate microhardness value had to be used instead of the bulk hardness suggested by CMY.[6] This is because real materials strain harden and have hard layers close to the surface. Therefore, for two rough surfaces undergoing plastic deformation

$$(A_r/A_a) = (P/H_c) \tag{10}$$

where $H_c \equiv$ appropriate microhardness[15,19] value of the softer surface in contact.

Mikic and Roca[16] derived an exact expression for the ratio of real area to the apparent area for two isotropic rough surfaces undergoing elastic deformation:

$$(A_r/A_a) = (\sqrt{2}P)/(E'm) \tag{11}$$

Hence, P/H_c and $(\sqrt{2}P)/(E'm)$ are suitable candidates for the values of dimensionless contact pressures. It can be seen from CMY,[6] Antonetti,[2] and Hegazy[3] that the most suitable dimensionless contact conductance parameter is

$$C_c = (\sigma/m) \cdot (h_c/k_s) \tag{12}$$

where $k_s \equiv$ harmonic mean thermal conductivity.

Dimensionless Forms of Contact Conductance Models

The next task was to plot the available models as C_c vs P/H_c or $(\sqrt{2}P)/(E'm)$, depending on whether the deformation is plastic or elastic, respectively.

It was shown by Sridhar[17] for the GW elastic model

$$C_c = \frac{(\alpha^{3/4}/24.95)\sqrt{I_1(\lambda)\text{erfc}(\lambda/\sqrt{2})}}{[1 - \sqrt{1/(2\sqrt{2}\pi^{3/2})\sqrt{\alpha}I_1(\lambda)}]^{1.5}}$$
$$\lambda = I^{-1}_{3/2}\left(\frac{18.72}{\alpha^{3/4}} \cdot \frac{\sqrt{2}P}{E'm}\right) \tag{13}$$

Modified GW Elastic Model

Similarly, the modified GW elastic contact model that incorporates the modified surface parameters used in Eqs. (1–3) is given by

$$C_c = \frac{[(\alpha - 0.8968)^{3/4}/22.6]\sqrt{I_1(\lambda)\text{erfc}(\lambda/\sqrt{2})}}{[1 - \sqrt{\sqrt{\pi}/(16\sqrt{3})}\sqrt{\alpha - 0.8968}I_1(\lambda)]^{1.5}}$$
$$\lambda = I^{-1}_{3/2}\left[\frac{16.94}{(\alpha - 0.8968)^{3/4}} \cdot \frac{\sqrt{2}P}{E'm}\right] \tag{14}$$

GW Plastic Model

The GW plastic contact model is given by

$$C_c = \frac{(\alpha^{3/4}/17.65)\sqrt{I_1(\lambda)\text{erfc}(\lambda/\sqrt{2})}}{[1 - \sqrt{1/(\sqrt{2}\pi^{3/2})\sqrt{\alpha}I_1(\lambda)}]^{1.5}}$$
$$\lambda = I_1^{-1}[(7.88/\sqrt{\alpha}) \cdot (P/H_c)] \tag{15}$$

It should be noted that another relationship relating rms surface slope $\sqrt{m_2}$ and m for Gaussian surfaces is required to reduce the GW model (both modified and unmodified) from the form presented in the previous section to the form in Eqs. (13–15) given by $m = \sqrt{m_2}/\sqrt{\pi/2}$. It is clearly seen from Eqs. (13–15) that the GW elastic and plastic models are not only a function of dimensionless contact pressure, but also a function of α.

The Mikic elastic model, the CMY plastic model, and the BGT elastic models are independent of any surface param-

eters, and C_c is a function of only the dimensionless contact pressure:

Mikic elastic model

$$C_c = \frac{1}{4\sqrt{\pi}} \frac{\exp(-\lambda^2/2)}{[1 - \sqrt{\tfrac{1}{4}}\,\mathrm{erfc}(\lambda/\sqrt{2})]^{1.5}}$$
$$\lambda = \sqrt{2}\,\mathrm{erfc}^{-1}\left(\frac{4\sqrt{2}P}{E'm}\right) \tag{16}$$

CMY plastic model

$$C_c = \frac{1}{2\sqrt{2\pi}} \frac{\exp(-\lambda^2/2)}{[1 - \sqrt{\tfrac{1}{2}}\,\mathrm{erfc}(\lambda/\sqrt{2})]^{1.5}}$$
$$\lambda = \sqrt{2}\,\mathrm{erfc}^{-1}\left(\frac{2P}{H_c}\right) \tag{17}$$

BGT elastic model

$$C_c = \frac{1}{2^{5/4}\pi^{5/4}} \cdot \frac{\exp(-\lambda^2/2)}{\sqrt{\lambda}\{1 - \sqrt{1/(2\sqrt{2\pi})[\exp(-\lambda^2/2)/\lambda]}\}^{1.5}}$$
$$\lambda = f^{-1}\left(2\sqrt{2\pi}\cdot\frac{\sqrt{2}P}{E'm}\right) \tag{18}$$

The WA elastic model is not only a function of the dimensionless contact pressure, but also a function of the parameter $\sigma^* = \sigma/(m \cdot l)$.

WA Elastic Model

The WA elastic in its dimensionless form is as follows

$$C_c = \frac{2\sigma^*}{5} \cdot \frac{\sqrt{I_{0,0}(\lambda) I_{1,1}(\lambda)}}{[1 - \sqrt{(\pi/5) I_{1,1}(\lambda)}]^{1.5}}$$
$$\lambda = I^{-1}_{3/2,1/2}\left(\frac{15}{4\sqrt{2}\sigma^*}\cdot\frac{\sqrt{2}P}{E'm}\right) \tag{19}$$

Quantitative Comparison of Previous Models

The third and final task was to estimate qualitatively the values of α and σ^* used in the GW and WA elastic model for the experimental data sets used in this investigation. Data obtained for isotropic surface pairs by Antonetti,[2] Hegazy,[3] and McWaid[4] covered a wide range of pressures varying from 0.15 to 8.9 MPa. Five materials were tested from soft aluminum 6061 (Al6061) to hard stainless steel 304 (SS304), with elastic modulli varying from 67 to 207 GPa. The data also covered a wide range of surface roughness with σ/m varying from 6 to 60 μm, T_c varying from 50 to 180°C, and k_s varying from 16 to 206 W/(m·K).

Table 5 shows a list of isotropic surfaces for which experimental test data were obtained by Hegazy,[3] Antonetti,[2] and McWaid.[4] Column 2 in Table 5 lists the values of σ/m for all the materials used in this work. The parameter σ/m is an important property of a surface that combines the surface roughness and the surface slope. The higher the value of σ/m, the rougher is the surface. Column 3 and 4 list values of σ^* and α. Values of σ^* for Antonetti's[2] data were not available. The bandwidth parameter α was not available for most of the surface pairs except for McWaid.[4] Examining columns 3 and 4 one can fix the ranges for σ^* (4–60) and α (5–15). With these ranges all the models can be plotted. The special functions and the integrals in all the models presented in this article were computed using *Mathematica*.[18]

Figure 1a shows a plot of all the elastic models except for the MT model. Most of the models lie close to each other

Table 5 Test pairs surface characteristics

Material	(σ/m), μm	$\sigma^* = (\sigma/m \cdot l)$	α
Ni200	08.20[a]	08.20	——
	08.81[b]	——	——
	17.86[b]	——	——
	18.01[b]	——	——
	18.05[a]	18.05	——
	22.55[a]	22.55	——
	24.62[b]	——	——
	41.80[a]	41.80	——
	59.83[a]	59.83	——
SS304	06.64[a]	06.64	——
	11.35[c]	04.54	5.70
	16.89[c]	06.76	9.34
	20.96[c]	08.38	14.30
	23.36[a]	23.36	——
	40.27[a]	40.27	——
	57.63[a]	57.63	——
Zr-Nb	11.11[a]	11.11	——
	15.43[a]	15.43	——
	32.55[a]	32.55	——
	44.05[a]	44.05	——
Zr-4	12.43[a]	12.43	——
	18.58[a]	18.58	——
	24.34[a]	24.34	——
	38.26[a]	38.26	——
Al-6061	14.32[c]	05.73	7.27
	21.08[c]	08.42	9.69
	28.31[c]	11.32	12.28

[a]Hegazy.[3] [b]Antonetti.[2] [c]McWaid.[4]

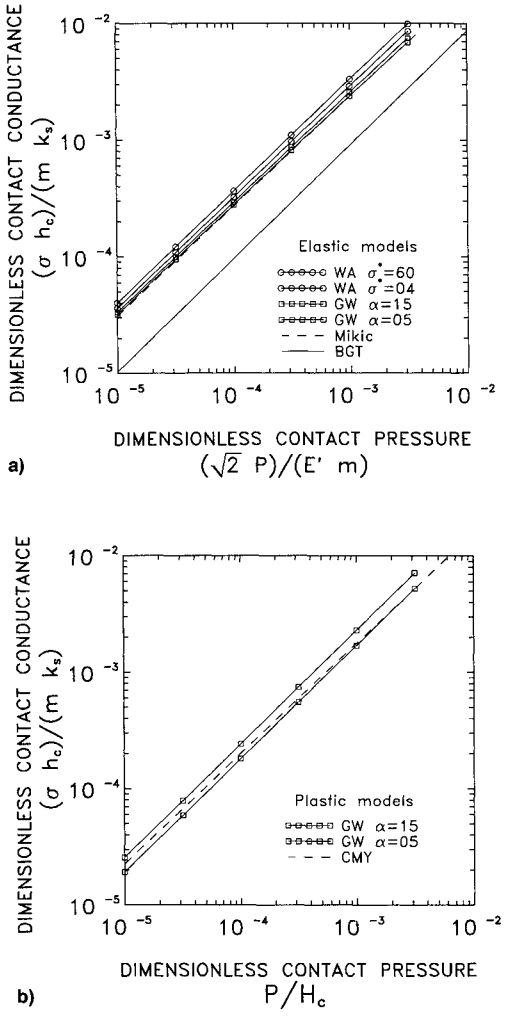

Fig. 1 Comparison of contact conductance model: a) elastic and b) plastic.

Table 6 Elastic and plastic properties of test pairs

Material	Elastic properties E, GPa	ν	Vickers microhardness $H_V = c_1 d_V^{c_2}$, GPa
Ni200	207	0.3	$H_V = 6.304 d_V^{-0.264}$ [a]
SS304	207	0.3	$H_V = 6.271 d_V^{-0.229}$ [a]
			$H_V = 7.361 d_V^{-0.280}$ [b]
Zr-Nb	96	0.3	$H_V = 5.884 d_V^{-0.267}$ [a]
Zr-4	96	0.3	$H_V = 5.677 d_V^{-0.278}$ [a]
Al-6061	67	0.3	$H_V = 1.110 d_V^{-0.00487}$ [b]

[a]Hegazy.[3] [b]Nho.[20]

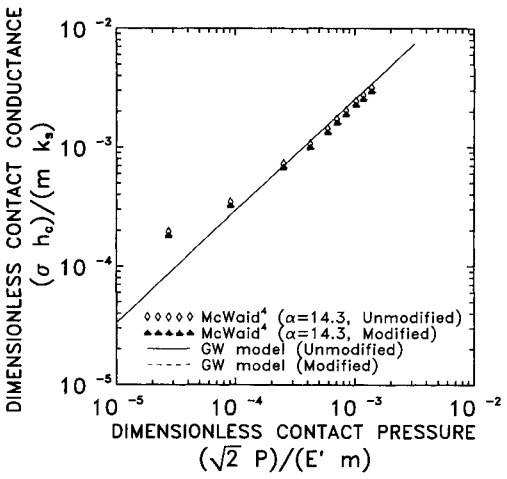

Fig. 2 Comparison of GW elastic model with a typical SS304 data set from McWaid[4] (unmodified and modified).

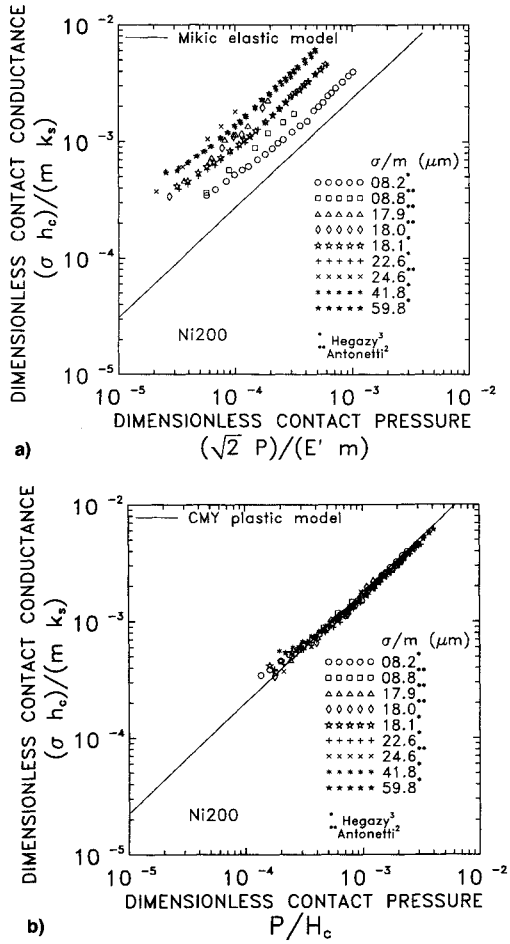

Fig. 3 Comparison of a) Mikic elastic model and b) CMY plastic model with Ni200 data.

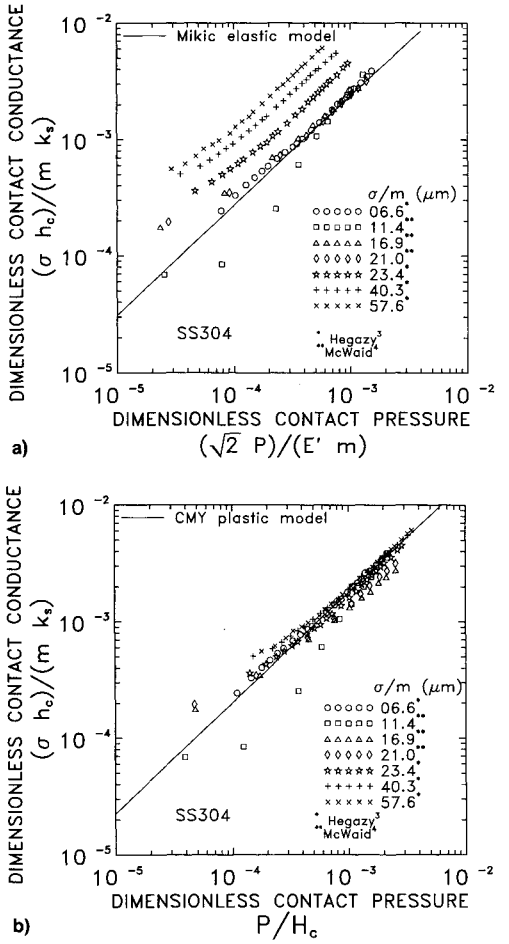

Fig. 4 Comparison of a) Mikic elastic model and b) CMY plastic model with SS304 data.

except for the BGT elastic model which lies well below. It can be seen that for a wide variation of σ^*, i.e., from 4 to 60, the effect on the WA model is minimal. The effect of variation of α from 5 to 15 on the GW model also seems to be very small. The GW and Mikic elastic models almost coincide when $\alpha = 5$ was chosen.

Similar trends can be seen in Fig. 1b where all the plastic models are plotted. The discrepancy between the CMY plastic model and the GW plastic model at $\alpha = 5$ could be due to a numerical error in the computation. It should be noted that all the models presented in Fig. 1 have not been modified.

It is clear that the GW and WA models require a value of α and σ^*, respectively, to be able to predict experimental data, and the BGT model seems to underpredict in comparison to other models. Therefore, in the present work in order to be able to compare different data from various workers on a single plot, the Mikic elastic model and CMY plastic model were considered to be most suitable.

Data Reduction

Experimental h_c is determined as follows:

$$h_c = (Q/A_a)/\Delta T_c \tag{20}$$

where $Q \equiv$ heat flow rate, A_a apparent contact area, and ΔT_c interface temperature drop.

This is nondimensionlized by multiplying it with $(\sigma/m)/k_s$. k_s was determined as follows:

$$k_s = \frac{2k_A k_B}{k_A + k_B} \tag{21}$$

where k_A and k_B are thermal conductivities of the upper and lower specimens. The thermal conductivities k_A and k_B for a

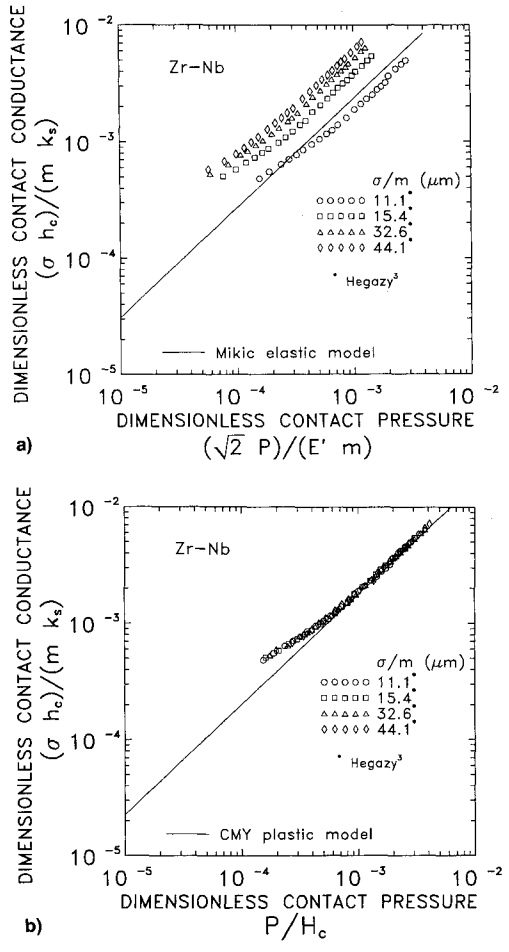

Fig. 5 Comparison of a) Mikic elastic model and b) CMY plastic model with Zr-Nb data.

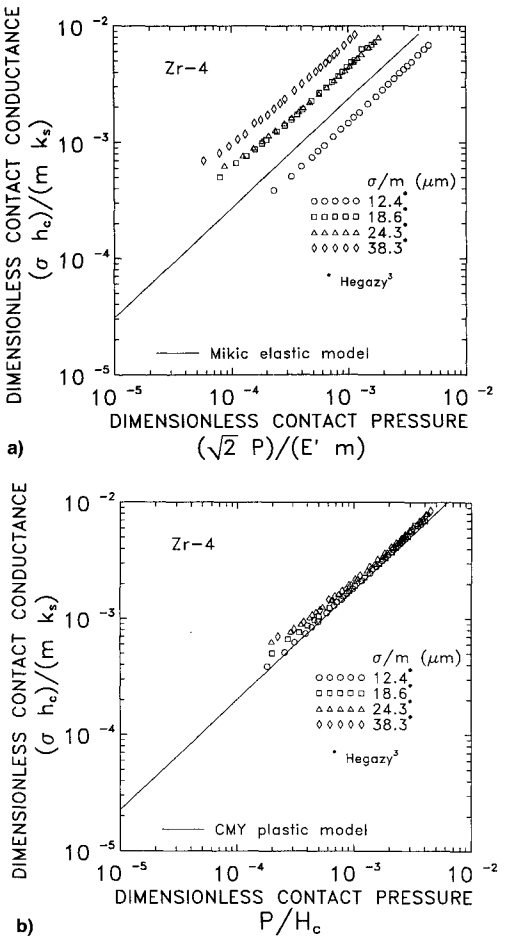

Fig. 6 Comparison of a) Mikic elastic model and b) CMY plastic model with Zr-4 data.

test pair were determined at T_c. Experimental uncertainty in measurements for the dimensionless contact conductance C_c was ±6.5% and ±12.4% for the Antonetti[2] and Hegazy[3] data, respectively. McWaid[4] did not provide values for uncertainty in his measurements.

Table 6 lists the elastic and plastic properties of all the materials used in this investigation. The dimensionless elastic contact pressure was determined using Eq. (11). The dimensionless plastic contact pressure was calculated using an explicit expression developed by Song and Yovanovich[19] for isotropic surfaces undergoing plastic deformation given by

$$(P/H_c) = (P/[c_1(1.62\sigma/m)^{c_2}])^{[1/(1+0.071c_2)]} \qquad (22)$$

Dimensionless plastic contact pressure depends on the surface parameter σ/m, where σ/m is in μm, and c_1 and c_2, which were obtained from careful microhardness measurements. Vickers correlation coefficients for all materials used here are reported in column 4 of Table 6. Since McWaid[4] did not perform microhardness tests on SS304 and Al6061, c_1 and c_2 obtained by Nho[20] was used to reduce his data.

To get a sense of the modified contact conductance model, a typical data set (SS304) from McWaid,[4] which had a value of $\alpha = 14.3$, was plotted against both the GW elastic and the modified GW elastic model.

Figure 2 shows plots of unmodified and modified GW elastic models against a typical data set from McWaid.[4] The rms differences between this typical data set and the two models (i.e., unmodified and modified versions), were 41.3 and 37.1%, respectively. It is very difficult to say whether the modified GW model is better, because if the first data point is discarded then the rms differences drop to 11.4% for the unmodified and 12.5% for the modified. This is consistent with what McWaid and Marschall[5] had observed. Hence, one can conclude that the effect of the modification is marginal. Because a number of data sets used in the present investigation do not have values of α, the modified contact conductance models have not been considered in this article.

Comparison of Data with Mikic Elastic and CMY Plastic Models

Figure 3a shows a comparison of the Mikic elastic model with nickel 200 (Ni200) data from Hegazy[3] and Antonetti[2] reduced assuming elastic deformation. For a wide range of surface roughnesses, i.e., σ/m varying from 8.2 to 59.8 μm, the agreement with the elastic model is not satisfactory. The rms differences range from 73 to 528%. Also, there is no definite order or arrangement of data with respect to the roughness parameter σ/m.

However, the same Ni200 data reduced assuming plastic deformation and compared with the CMY plastic model in Fig. 3b show excellent agreement, and the rms differences range from 5.4 to 13.5%. It can be seen that Antonetti's[2] data sets show very little low load deviation and have rms differences less than 7.3%.

Figure 4a shows the comparison of the SS304 data obtained by Hegazy[3] and McWaid[4] with the Mikic elastic model. The data have been obtained for a wide range of surface roughness values with σ/m varying from 6.6 to 57.6 μm. The first four data sets having σ/m values of 6.6, 11.4, 16.9 and 21.0 μm compare quite well with the Mikic elastic model, and the rms differences are 11.3, 29.9, 53.4, and 47.4%, respectively. The larger rms differences seen in the McWaid[4] SS304 data is due to the large deviation of the few low load data points. The set that has an rms difference of 29.9% has only three data points with percent differences greater than 30. Similarly, the data sets with σ/m of 16.9 and 21.0 μm have in total about

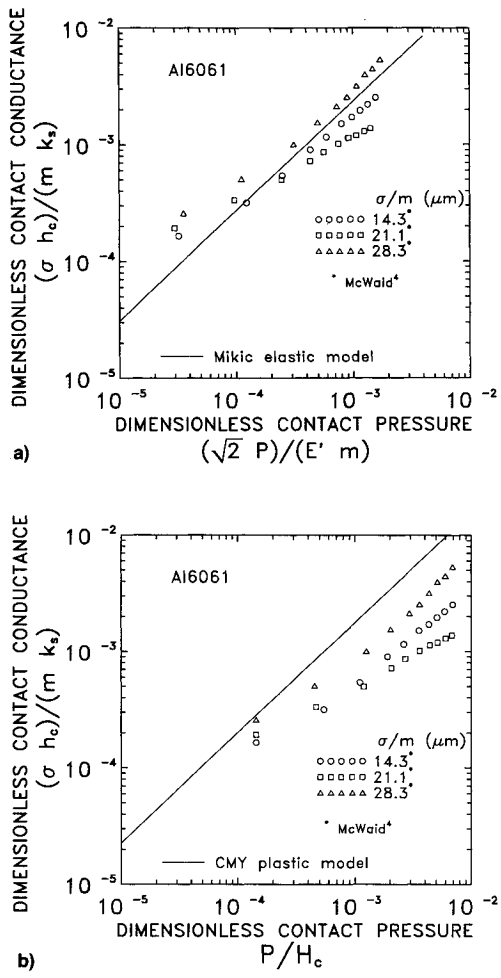

Fig. 7 Comparison of a) Mikic elastic model and b) CMY plastic model with Al6061 data.

three points that have percent differences greater than 20. The data sets with σ/m equal to 23.4 μm and greater are well above the Mikic elastic model, with rms differences ranging from 107 to 372%. It can also be seen that the data sets are arranged in a definite order with surfaces of higher σ/m moving further away from the model. For the last three data sets the type of deformation seems to be quite different from elastic.

Figure 4b shows the same set of SS304 data reduced assuming plastic deformation. The comparison is very good, especially for the data sets with values of σ/m equal to or greater than 23.4 μm. The rms differences for the data sets with the CMY plastic model as σ/m is increased in ascending order are 8.9, 35.2, 36.0, 38.4, 11.0, 21.0, and 20.2%. Except for the first data set from Hegazy,[3] all the other data sets show a considerable deviation from the model at light loads.

Figure 5a shows a comparison of the zirconium alloy Zr-Nb data with the Mikic elastic model. The smoothest pair seems to agree well with the model and has an rms difference of 18.7%. The remaining data sets are well above this and the rms differences range from 76 to 170%. Figure 5b shows the same data reduced assuming plastic deformation. Except for the large low load deviation for the first few data points, the agreement is quite good with rms differences in the range of 16 to 23%.

Figure 6a shows the other zirconium alloy (Zr-4) compared with the elastic model. A large deviation is observed for all data sets except for the smoothest pair, which recorded an rms difference of 36.3%. In Fig. 6b the CMY plastic model and the Zr-4 data obtained by Hegazy[3] can be seen. Agreement is good, even though the rougher pairs exhibit considerable low load deviation. The calculated rms differences as roughness was increased in ascending order were 6.3, 13.1, 26.0, and 25.0%.

Figure 7a shows the McWaid[4] Al6061 data reduced assuming elastic deformation. There is considerable scatter in the experimental data, and the calculated rms differences as roughness was increased in ascending order were 31.8, 56.3, and 59.1%. When the same data were reduced assuming plastic deformation, the comparison with the CMY plastic model (Fig. 7b) is not satisfactory, indicating that the mode of deformation for Al6061 could be different from plastic. The data do not seem to come together like the other data. The rms differences range from 50 to 70%. It should be noted that Nho's[20] hardness data were used to reduce McWaid's[4] Al6061 data.

Discussion and Comparisons

It is clear from the Ni200 data sets that for a wide variation of surface roughness, i.e., σ/m varying from 8 to 60 μm, the mode of deformation is plastic. Comparison of the nine sets of data with the CMY plastic model yielded the largest value of rms difference of 13.5%. Whereas comparing the same data with the elastic model yielded rms differences ranging from 73 to 530%.

When the first four data sets of SS304 having σ/m ranging from 6.6 to 21.0 μm were compared with the Mikic elastic model, it yielded rms differences of 11.3, 29.9, 53.4, and 47.4%. The corresponding values when the same four data sets were compared with the CMY plastic model were 8.9, 35.2, 36.0, and 38.4%. It is very difficult to conclude whether these pairs underwent elastic or plastic deformation during loading. It is quite possible that these four surface pairs underwent elastoplastic deformation.

The type of deformation for the zirconium alloy Zr-Nb is questionable only for the smoothest pair (σ/m = 11.1 μm), where the rms differences for the elastic and plastic cases were 18.7 and 23.2%, respectively. Similar to the four smooth pairs of SS304 the type of deformation for this surface pair could be elastoplastic.

It is almost certain from the comparisons for the Zr-4 surface pairs tested by Hegazy[3] that the deformation mode is fully plastic.

Even though the smoothest Al6061 pair tested by McWaid[4] appear to be deforming elastically, one cannot be very certain about it. The data show a large scatter and are arranged in a disorganized manner. The other two rougher pairs of Al6061 do not compare well with either the elastic or the plastic models.

Concluding Remarks

Data from four different materials, viz., Ni200, SS304, Zr-Nb, Zr-4 and Al6061, have been reduced to a dimensionless form for the first time, assuming both elastic and plastic deformation and compared with the Mikic elastic and the CMY plastic models. It is more or less clear that smoother pairs deform elastically and rougher pairs plastically. The comparisons with the plastic model for most of the data sets are very good and the data come together in the dimensionless plot. This clearly shows the need to use the appropriate microhardness value while reducing the data.

The value of σ/m at which there is significant plastic deformation as compared to elastic deformation seems to be different for the different materials considered in this investigation. The data sets that compare well with both elastic and plastic models indicate that the type of deformation associated with them may be elastoplastic. Hence, there is need for an elastoplastic contact conductance model. An elastoplastic contact conductance model would avoid the need to assume a priori a type of deformation for the data sets.

Significant light load deviation of data sets are seen for the data obtained by Hegazy[3] and McWaid.[4] Therefore, there is

a need to examine this aspect both from an experimental as well as analytical point of view.

It is very difficult to conclude with the present data sets where the approximate change takes place from elastic to plastic deformation for the Al6061 surfaces. There is a need to obtain more experimental data.

Acknowledgment

The authors acknowledge the support of the Natural Science and Engineering Research Council of Canada under Grant A7445.

References

[1]Johnson, K. L., *Contact Mechanics*, Cambridge Univ. Press, Cambridge, England, UK, 1985.

[2]Antonetti, V. W., "On the Use of Metallic Coatings to Enhance Thermal Contact Conductance," Ph.D. Dissertation, Univ. of Waterloo, Waterloo, Ontario, Canada, 1983.

[3]Hegazy, A. A., "Thermal Joint Conductance of Conforming Rough Surfaces," Ph.D. Dissertation, Univ. of Waterloo, Waterloo, Ontario, Canada, 1985.

[4]McWaid, T. H., "Thermal Contact Resistance Across Pressed Metal Contact in a Vacuum Environment," Ph.D. Dissertation, Univ. of California, Santa Barbara, Santa Barbara, CA, 1990.

[5]McWaid, T. H., and Marschall, E., "Application of the Modified Greenwood and Williamson Contact Model for the Prediction of Thermal Contact Resistance," *Wear*, Vol. 152, No. 2, 1992, pp. 263–277.

[6]Cooper, M. G., Mikic, B. B., and Yovanovich, M. M., "Thermal Contact Conductance," *International Journal of Heat and Mass Transfer*, Vol. 12, No. 3, 1969, pp. 279–300.

[7]Greenwood, J. A., and Williamson, J. B. P., "Contact of Nominally Flat Surfaces," *Proceedings of the Royal Society of London*, A295, No. 1442, 1966, pp. 300–319.

[8]Mikic, B. B., "Thermal Contact Conductance; Theoretical Considerations," *International Journal of Heat and Mass Transfer*, Vol. 17, Feb. 1974, pp. 205–214.

[9]Bush, A. W., Gibson, R. D., and Thomas, T. R., "The Elastic Contact of a Rough Surface," *Wear*, Vol. 35, No. 2, 1975, pp. 87–111.

[10]Sayles, R. S., and Thomas, T. R., "Thermal Conductance of a Rough Elastic Contact," *Applied Energy*, Vol. 2, 1976, pp. 249–267.

[11]Whitehouse, D. J., and Archard, J. F., "The Properties of Random Surfaces of Significance in Their Contact," *Proceedings of the Royal Society of London*, A316, No. 1524, 1970, pp. 97–121.

[12]Onions, R. A., and Archard, J. F., "The Contact of Surfaces Having a Random Structure," *Journal of Physics D: Applied Physics*, Vol. 6, No. 3, 1973, pp. 289–304.

[13]Majumdar, A., and Tien, C. L., "Fractal Network Model for Contact Conductance," *Journal of Heat Transfer*, Vol. 113, Aug. 1991, pp. 516–525.

[14]Majumdar, A., and Bhushan, B., "Fractal Model of Elastic-Plastic Contact Between Rough Surfaces," *Journal of Tribology*, Vol. 113, Jan. 1991, pp. 1–11.

[15]Yovanovich, M. M., and Hegazy, A., "An Accurate Universal Contact Conductance Correlation for Conforming Rough Surfaces with Different Micro-Hardness Profiles," AIAA Paper 83-1434, June 1983.

[16]Mikic, B. B., and Roca, R. T., "On Elastic Deformation of Rough Surfaces in Contact," Dept. of Mechanical Engineering, Massachusetts Institute of Technology, Cambridge, MA.

[17]Sridhar, M. R., personal communication to M. M. Yovanovich, Univ. of Waterloo, Waterloo, Ontario, Canada, 1993.

[18]*Mathematica, A System for Doing Mathematics by Computer*, Version 2 for DOS, Wolfram Research, Inc., Champaign, IL, 1988, 1991.

[19]Song, S., and Yovanovich, M. M., "Relative Contact Pressure: Dependence on Surface Roughness and Vickers Microhardness," *Journal of Thermophysics and Heat Transfer*, Vol. 2, No. 1, 1988, pp. 43–47.

[20]Nho, K. M., "Experimental Investigation of Heat Flow Rate and Directional Effect on Contact Conductance of Anisotropic Ground/Lapped Interfaces," Ph.D. Dissertation, Univ. of Waterloo, Waterloo, Ontario, Canada, 1990.